ISPRS Journal of Photogrammetry and Remote Sensing 68 (2012) 95–111

Contents lists available at SciVerse ScienceDirect

ISPRS Journal of Photogrammetry and Remote Sensing

journal homepage: www.elsevier.com/locate/isprsjprs

Mathematical morphology-based generalization of complex 3D building models incorporating semantic relationships

Junqiao Zhao [a,b], Qing Zhu [b,*], Zhiqiang Du [b], Tiantian Feng [a], Yeting Zhang [b]

[a] Tongji University, Department of Surveying and Geo-Informatics, Siping Road 1239, Shanghai, China
[b] Wuhan University, State Key Laboratory of Information Engineering in Surveying, Mapping and Remote Sensing, Luoyu Road 129, Wuhan, China

ARTICLE INFO

Article history:
Received 25 July 2011
Received in revised form 6 January 2012
Accepted 11 January 2012
Available online 15 February 2012

Keywords:
Generalization
Complex 3D building
Mathematical morphology
Levels of Detail
Semantic relationships

ABSTRACT

A complex 3D building model contains a detailed description of both its appearance and internal structure with authentic architectural components. Because of its high complexity and huge data volumes, using a less detailed representation for the distant visual application of such a model is preferable. However, most mesh simplification algorithms cannot preserve manmade features of such models, and the existing 3D generalization algorithms are mainly proposed for regular-shaped buildings. More importantly, neither method can consistently express geometry, topological relations, and semantics in multiple discrete Levels of Details (LoDs). This paper presents a novel mathematical morphology-based algorithm that generalizes the complex 3D building model in a unified manner using the following steps: (1) semantic relationships between components, which reflect structural connectivity in the building at a certain LoD, are defined and extracted; (2) semantically connected components are merged and trivial geometric features of the components are eliminated simultaneously, with semantics associated with components then updated according to the merging; and (3) post-process is carried out to further reduce the redundancy of facets. The semantic relationships extracted ensure the proper generalization of topological relations and semantics of building components, and mathematical morphological operations implemented in the algorithm are capable of handling closed two-manifold components of various shapes. Experiments on both complex 3D building models in the classical Chinese style and prismatic 3D city models prove the effectiveness of the proposed method.

1. Introduction

The detailed 3D modeling of building has become increasingly important in various GIS applications such as building information modeling (BIM), emergency management, and digital documentation of cultural heritage. Such building models are characterized by highly complicated appearances, intricate internal structures, huge volumes of data, and complex relations between components (Du et al., 2008). Although the tremendous improvement in the computational power of modern hardware has abided by Moore's Law, it still could not catch up with the explosive growth of 3D data (Gobbetti et al., 2008). Additionally, the complexity of building components prohibits users from easily acquiring geometrical and structural knowledge. As a result, Levels of Details (LoDs) should be created, on the one hand, to alleviate the pressure on the visualization system and, on the other hand, to raise the efficiency of spatial cognition by reducing the information density (Sester, 2007; Gröger et al., 2008).

In this paper, the generalization is defined as the process that automatically creates a series of discrete LoDs from a complex 3D building model. Most of the existing 3D generalization methods are extended from 2D cartographic generalization and are proposed for regular prismatic building models rather than models with internal structures and smooth surfaces (Meng and Forberg, 2006; Sester, 2007). Another method that could produce LoDs is mesh simplification in the field of computer graphics. The topology-based approach could even merge multiple models and thereby eliminate the complexity of aggregate models (Luebke et al., 2003). However, this method is not suitable for maintaining the characteristics of buildings, such as parallel and perpendicular. More importantly, neither method generalizes topological relations and semantics according to the semantic relationships that indicate the correct structural connectivity between building components. Thus the consistent generalization of geometry, topological relations, and semantics cannot be achieved.

* Corresponding author at: Wuhan University, State Key Laboratory of Information Engineering in Surveying, Mapping and Remote Sensing, Luoyu Road 129, Wuhan, China. Tel.: +86 27 68778322; fax: +86 27 68778229.
E-mail addresses: johnzjq@gmail.com (J. Zhao), zhuqing@lmars.whu.edu.cn (Q. Zhu), duzhiqiang@lmars.whu.edu.cn (Z. Du), fengtiantian@tongji.edu.cn (T. Feng), zhangyeting@lmars.whu.edu.cn (Y. Zhang).

0924-2716/$ - see front matter © 2012 International Society for Photogrammetry and Remote Sensing, Inc. (ISPRS) Published by Elsevier B.V. All rights reserved.
doi:10.1016/j.isprsjprs.2012.01.002

This paper presents a novel automatic generalization method incorporating the semantic relationships between components. The merging of semantically connected components considering structural connectivity and semantic constrains prevents the aggregation of structurally separated or heterogeneous components. By exploring the generality provided by the 3D Minkowski sum and the 3D Boolean operation, the method could apply to complex building components of both regular and irregular shapes.

The remaining parts of this paper are organized as follows: Section 2 addresses the related work. In Section 3, the complexity of complex 3D building models in geometry, topological relations, and semantics is analyzed; based on this analysis, the derivation of LoDs of complex 3D building models incorporating semantic relationships are established. Section 4 proposes the implementation details of the proposed generalization algorithm. The experimental results are illustrated in Section 5. The analysis and discussion are presented in Section 6. Finally, Section 7 concludes the paper and discusses future directions.

2. Related work

The state-of-the-art research on reducing the complexity of 3D building models can be divided into two categories: one is the mesh simplification that aims at the process of general 3D models, and the other is the 3D generalization proposed specifically for 3D building models.

2.1. Mesh simplification of 3D models

Since the introduction of LoD in 1976, a large number of simplification algorithms have been proposed (Luebke et al., 2003). The basic concept behind these algorithms is the use of error metrics to evaluate the impact of the simplification operation on the mesh. However, such methods are not good at preserving the characteristics of buildings. It is also known that a heuristic strategy is not suitable for simplifying aggregate models with components of various sizes (Cook et al., 2007).

To address the above-mentioned shortcomings, the feature-based simplification is proposed. The main idea is to extract the features defined in a model; the model is then simplified through the gradual elimination of features. Ribelles et al. (2001) proposed an algorithm that uses split planes to divide the model space to detect and eliminate protruding and concave features. Jang et al. (2006) introduced a loop-based method that segments the mesh based on detected loops to construct a feature hierarchy. Recently, a novel method was proposed that fits the outline of the model with curves and contours (Mehra et al., 2009). More extensive reviews of feature-based simplification can be found in Babic et al. (2008) and Thakura et al. (2009). This kind of method is proposed usually for a specified type of models. Definition of the features is therefore needed for other models, which reduces the applicability of these methods. Furthermore, aggregation of models is not supported.

The aggregation of 3D models requires the simplification of topological relations. El-Sana and Varshney (1998) introduced the extended α-shapes to identify holes and cracks in a model, and the $L-\infty$ cube is employed to fill these areas using sweeping. This method shows good results for the elimination of genus and concave/convex features, but the proper merging of different models is not mentioned. Simplification algorithms using vertex-pair collapse and vertex clustering could also modify the topological relations of 3D models (Garland and Heckbert, 1997; Luebke and Erikson, 1997). However, they can hardly guarantee a smooth connection between models, and non-manifold cases would probably arise in the results. Another kind of method first converts the model to a voxel-based representation. Then, smoothing filters defined in voxel space are performed to achieve topological simplification and model repair. After this, the model is reconstructed to mesh-based representation (Nooruddin and Turk, 2003). This method can simplify aggregate models due to its unified handling of the geometry and the topological relations. However, the conversion between a polygonal mesh and a voxel-based representation introduces notably distortions on the surface.

2.2. Generalization of 3D building models

Generalization is a traditional research topic in the field of cartography. Methods of 2D generalization have been extended to 3D, and specified algorithms for 3D buildings are proposed as well.

Kada (2002) constructed a constraint model for buildings based on the relations between patches (e.g., coplanar, vertical, and parallel) on the surface. Features of the building model are then simplified using edge-collapse with the constraints. This method can eliminate trivial features in a building while the characteristics of the model can be maintained. However, it cannot merge multiple building parts. Inspired by Ribelles et al. (2001), Thiemann and Sester (2004) implemented a similar method to split a building into several meaningful parts (a roof, windows, and so on), and then the building is generalized by eliminating the building parts. This method cannot merge different models, and the detection of complex features using multiple split planes is expensive. Anders (2005) extended two generalization operators, namely aggregation and typification, from 2D to 3D building groups. This method projects the 3D model to several orthogonal 2D planes. Generalization is then implemented in 2D space, and finally, the 3D model is rebuilt from 2D space. This method applies only to prismatic building models. Rau et al. (2006) proposed a feature-resolution-based pseudo-continuous LoD. It employs the merging of polyhedral models and the simplification of walls and roofs to construct a model with a particular feature resolution. However, this method requires the pre-assignment of building parts, (e.g., windows, walls, and so on) in the model. To generalize 2D and 3D building models at multiple scales, a scale-space-based generalization was proposed (Mayer, 2005; Forberg, 2007). The purpose of this method is to establish a causal link between the scale and the representation of features in the model. During implementation, this method gradually shifts edges (in the 2D case) or facets (in the 3D case) to their opposite parallel edges or facets. The squaring of the model is thus mandatory. However, this cannot be applied to complex 3D building models. Additionally, this approach simply merges the spatially adjacent models without considering their relationships.

Kada (2007) proposed a cell-based generalization method that splits the 3D building model into multiple cells according to its ground plan. The cell is then simplified and the generalized 3D building is finally constructed by merging the cell and the rebuilt roof. For the generalization of building models defined in CityGML, Fan et al. (2009) proposed a series of generalization operators based on the constraints provided by the semantics associated with the geometry; these are the shell extraction, simplification of the building ground plan, and the typification of windows. Both of the cell-based and CityGML-based methods utilize the 2D ground plan and the characteristics of the building, thus can produce promising results for regular-shaped 3D buildings. However, the ground plan cannot assist with the generalization of complex 3D buildings.

Guercke et al. (2010) proposed a typification method for generalizing curved tile surfaces in complex 3D building models. First, this method approximates the distribution of tiles using a piecewise parabolic interpolation. The tiles are then rearranged and resized based on the interpolation to produce different LoDs.

However, this method mainly focuses on repeated units. In addition, convex-hull-based and voxel-based generalization approaches were also proposed (Glander and Döllner, 2007). Nevertheless, the convex-hull is too coarse for presenting buildings, and the voxel-based method has similar drawbacks, as discussed in Section 2.1.

In sum, both mesh simplification and 3D building generalization approaches can partially solve the problem. Topological simplification can simplify the geometry and the topological relations of a complex aggregate model, but most of these methods cannot maintain the characteristics of buildings. Feature-based simplification can eliminate the trivial details of a building while keeping its dominant features. However, it always requires a specified definition of features, and the merging of models is not supported. The 3D building generalization approach accounts for the characteristics of a building. However, the drawback to this approach is that it is proposed mainly for regular-shaped buildings (i.e., 2.5D), and it cannot generalize component-based 3D building models. Therefore, LoDs of complex 3D building models are often created interactively, which is time consuming and error-prone. It is necessary to derive a method that can automatically create multiple abstractions for complex 3D building models and can also maintain the consistency of geometry, topological relations, and semantics.

3. LoDs of complex 3D building models

3.1. Definition

A complex 3D building model is a type of aggregate model assembled from thousands of building components. The abstraction of such models can vary depending on the application requirements. For fly-through visualization, the elimination of imperceptible primitives or the approximation of the appearance is appropriate (Mehra et al., 2009; Zhu et al., 2009). However, for other applications, such as BIM, observation, and query of both the outside and inside of the building are needed; such specifics can help users understand the detailed composition of a building. In this case, not only the geometric appearance but also the topological relations and the semantics associated with the components should be handled during the generalization in order to provide appropriate levels of abstraction for cognition and to achieve the correct causal links between LoDs. Therefore, the LoD of complex 3D building models can be defined as the unified multi-level abstraction of geometry, topological relations, and semantics:

$$LoD(M) = LoD(G, T, S)$$

where G represents the geometry of the components in the model, T represents the topological relations of the components in the model, and S represents the semantics associated with the components in the model (i.e., materials, taxonomy, and so on).

The complexity of the geometry can be evaluated based on the following three aspects. (1) The geometry of a component contains rich features. As shown in Fig. 1, in addition to the necessary structural joints, a large number of decorative features are also included. In the abstract expression of the component, trivial features should be eliminated. (2) The geometry of a component is composed of numerous facets, which lead to the high cost of real-time rendering. In the generalization, redundant facets must be simplified. (3) Building components usually differ in size and may possess irregular shapes. Thus, the heuristic mesh simplification or the 3D generalization methods proposed for regular-shaped models cannot be applied. The former may completely remove small components (which undermines the integrity of the building), and the latter cannot handle irregular features.

The simplification of topological relations is a unique part of the generalization of complex 3D building models. The existed topological relations between building components are "meet" and "disjoin" as defined by Egenhofer and Robert (1991). However, the same topological relation of component-pairs can express different meanings in the structural domain. These relations, termed as semantic relationships in this paper, should be recognized and properly handled during the generalization in order not to violate the rules of the building structure. There are two typical relationships: one is mortise-and-tenon-like relationship, in which connected components are joined by the nested mortise and tenon features, but "meet" components are not necessarily connected (as shown in Fig. 2). This relationship can be mainly found in timber frame buildings and structures with bolted joints. The other is masonry-like relationship. In this case, components are represented as repeated units, such as the tiles shown in Fig. 3. In this

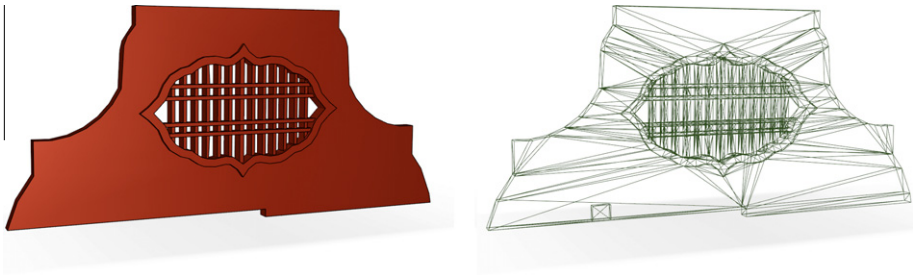

Fig. 1. The Gong Yan Bi: a typical component with rich features and 1982 triangles (left, displayed in shaded mode; right, displayed in wireframe mode).

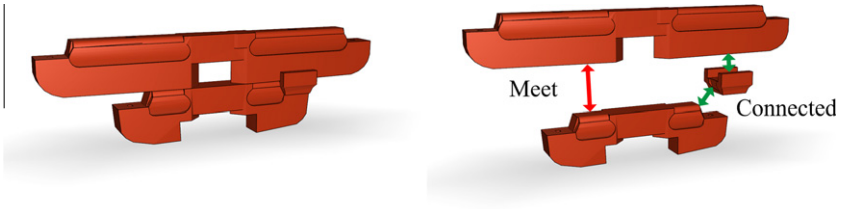

Fig. 2. Gong and Dou: illustration of the relationships between timber frame components (left, the original model; right, the exploded view illustration).

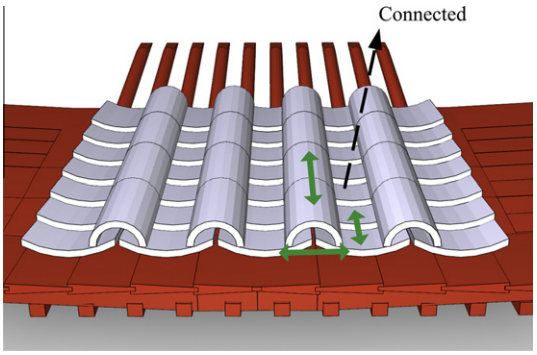

Fig. 3. Tiles and cornice board: a collection of components composed of different materials.

type of relationship, contiguous components, as indicated by the arrows, are connected.

The semantics of complex 3D buildings can vary depending on their different contexts. In this paper, the main consideration is the building structure, specifically the material and the structural taxonomy. The material comprises an important part of the semantic relationships between components. It constrains the generalization of topological relations because components made up of different materials (such as the tiles and timber cornice boards shown in Fig. 3) should not be merged. Otherwise, a new material must be derived. The taxonomy attributes of components are especially important for query-related applications in which attributes should match the geometry at different LoDs. As a result, the attribute of the aggregated component must be updated to the correct level in the taxonomy hierarchy.

3.2. LoDs derivation

To automatically generate LoDs for complex 3D building models that meet the above definition, a feature-independent and non-heuristic method should be adopted. The linear scale space defined in 2D image space provides a mathematically rigorous way to create multi-level abstraction, in which the characteristics of specific pixel clusters in the image do not have to be considered (Lindeberg, 1994). Inspired by this theory, one can assume a feature-removal kernel $K(t)$ that works on the surface of 3D models. Each component is "convoluted" by the kernel of size t, termed as scale parameter in the following paragraphs. Subsequently, all the geometric features that are smaller than the kernel are eliminated, but all the larger ones are retained. The semantic relationships between components can be extracted based on the "convolution" and the material attributes the components hold. If two homogeneous components intersect after "convolution", this indicates that these components are probably connected and will then be merged. Finally, semantics associated with the components are updated based on certain abstraction rules according to the merging. This method does not require the explicit definition of features, and generalizes the geometry, the topological relations, and the semantics of the building components under global control, thus avoids the drawbacks of both feature-based and heuristic-based methods.

Fig. 4 demonstrates the derivations of LoDs at different scale parameters. Let LoD_i be the generalized model produced at scale parameter i. As i increases, the level of generalization becomes higher. Let $\{G_x \mid x \in A, \ldots, Z\}$ represent the component geometry in the building, $\{f_x \mid x \in \mathbb{N}\}$ represent features within a component, $\{m_x \mid x \in a, \ldots, z\}$ represent the polygonal mesh that compose the component and $\{S_x \mid x \in \mathbb{N}\}$ represent the semantics associated with the component. In the generalization from LoD_i to LoD_{i+1}, features f_0 in geometry G_A, f_6 in geometry G_C and f_8 in geometry G_D are eliminated because they are less than or equal to the kernel $K(i+1)$ at the scale parameter $i+1$. In addition, the polygonal mesh is also simplified to reduce redundancy (i.e., $m_a \rightarrow m_e$). For the generalization of topological relations, G_C and G_D are merged into G_C because the two models are semantically connected, which means the distance between the two models is less than or equal to the kernel $K(i+1)$ and their semantics allow for the merging. It can be observed that the semantics associated with G_C are updated according to the semantic hierarchy shown in the right-hand figure (i.e., S_5, $S_5 \rightarrow S_2$).

Generalization from LoD_{i+1} to LoD_{i+2} is similar. At the highest level of abstraction, all the features in the geometry are eliminated and all the semantically connected components are merged, but the overall shape and structure of the building is delivered. In the following sections, an automatic generalization algorithm that implements the ideas noted above will be presented.

4. Algorithm description

A way to eliminate model features in scale space has been proposed by Mayer (2005) and Forberg (2007). However, moving parallel facets against their opposites is suitable only for orthogonal

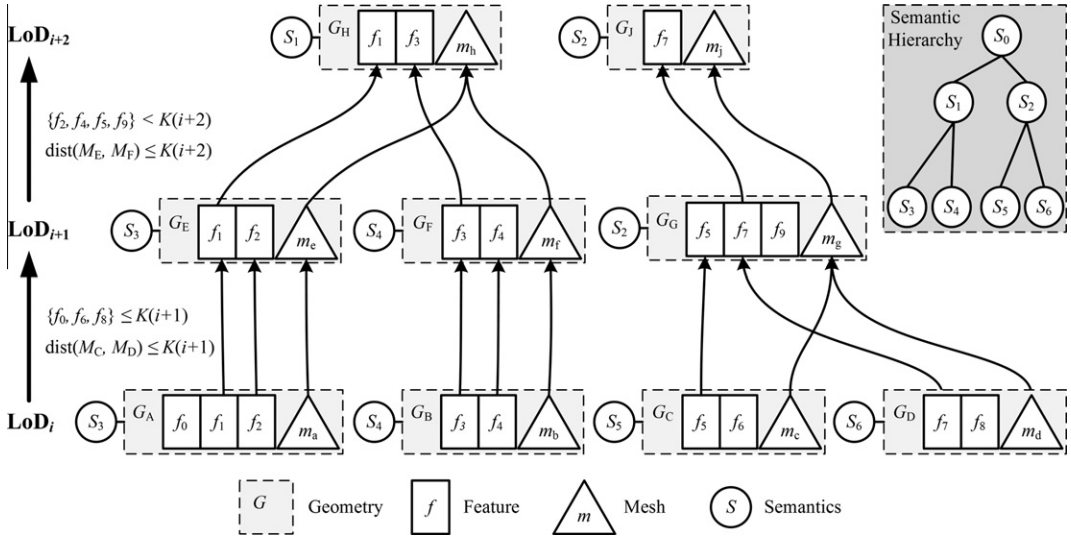

Fig. 4. The derivation of LoDs at different scale parameters.

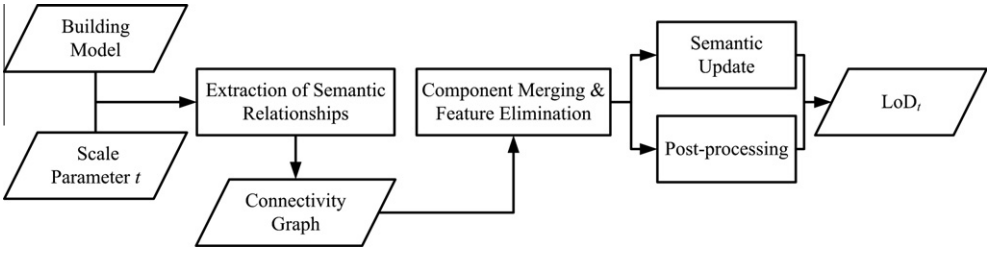

Fig. 5. Flow chart of the algorithm.

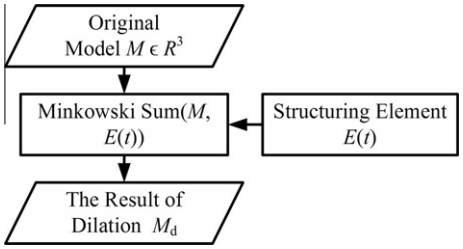

Fig. 6. Flow chart of the dilation algorithm.

building structures and this method does not take into account the generalization of topological relations and semantics of models. To overcome these shortcomings, this paper introduces a mathematical morphology-based approach that can handle closed two-manifold meshes of both regular and irregular shapes. In the first step, the morphological operators and the collision detection are combined to extract semantic relationships between components. During this process, a connectivity graph is used to record the extracted relationships. The connectivity graph is an undirected graph in which nodes represent components and links represent connections between components with semantic constraints. Subsequently, 3D Boolean operators and morphological operators are employed to merge semantically connected components while eliminating trivial grooves, holes, and protrusions from within the component. In the next step, the semantics of the newly created components are updated, and post-processing is employed to simplify the redundant facets. The flow chart of the algorithm is shown in Fig. 5.

4.1. Morphology operators

Morphological operators, including dilation, erosion, opening, and closing, are implemented based on the Minkowski sum and the Boolean operation in 3D. The Minkowski sum of two point sets is defined as follows: given two point sets P and Q in nD space, their Minkowski sum $P \oplus Q$ is a new point set defined as $\{p+q \mid p \in P, q \in Q\}$. Fogel and Halperin (2007) gave an efficient algorithm to calculate the Minkowski sum of a convex polyhedron, and the application of Minkowski sums for collision detection is also demonstrated. Peternell and Steiner (2007) proposed a convolution-based implementation of the Minkowski sums of triangle meshes that illustrates the suitability of this method for complex 3D models. Damen et al. (2008) first employed the 2D Minkowski sum for automatic map generalization. However, to our knowledge, the use of Minkowski sums for the generalization of 3D building models is still rare.

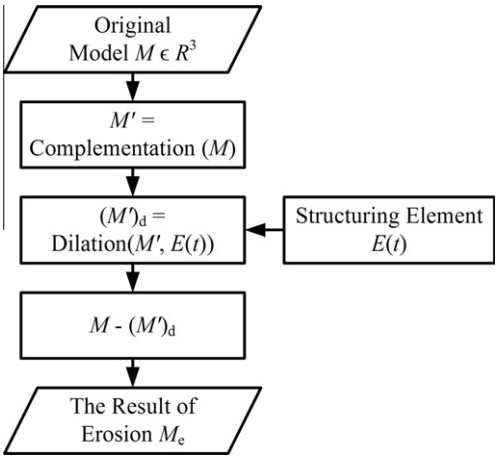

Fig. 8. Flow chart of the erosion algorithm.

4.1.1. Dilation

Dilation is the basic morphological operator. The dilation of model A by structural element B is defined as $A \oplus B = \bigcup_{b \in B} A_b$. This process expands all the primitives of A by the shape of B, which can be achieved using a 3D Minkowski sum (as shown in Fig. 6). The structural element $E(t)$ used in this paper is defined as a cube with the size of scale parameter t. The results in Fig. 7 show that dilation by $E(t)$ could preserve the manmade features of the models and expand the model equidistantly which help to accurately extract the relationships between components.

4.1.2. Erosion

The erosion of model A by structural element B is defined as $A \ominus B = \bigcap_{b \in B} A_{-b}$. This process erodes all the primitives of A by the shape of B and can be achieved using the 3D Minkowski sum and the 3D Boolean operation (as shown in Fig. 8). M', the complement

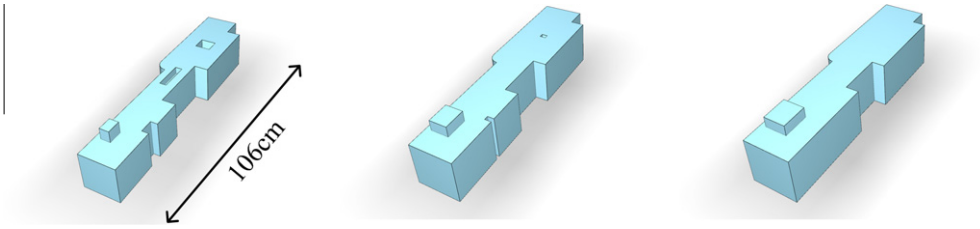

Fig. 7. Illustration of the result of the dilation (left, the original model; middle, the dilation result at scale parameter 4 cm; right, the dilation result at scale parameter 6 cm).

of the original model, is first calculated. Then, $(M')_d$, the result of dilation of M' by $E(t)$, is obtained using the Minkowski sum. Finally, the erosion of M is calculated by subtracting $(M')_d$ from M. Examples are shown in Fig. 9. One can also achieve the same result by first inverting the normal of every facet and dilating the model using $E(t)$.

4.1.3. Opening and closing

Opening and closing can be realized based on the consecutive execution of dilation and erosion. The opening and closing of model A by structural element B are defined as $A \circ B = (A \ominus B) \oplus B$ and $A \bullet B = (A \oplus B) \ominus B$. Opening can eliminate small protrusions and connections, while closing can fill grooves and holes in a model. The results of opening and closing are shown in Figs. 10 and 11. In this paper, closing is used more frequently because it can better preserve the outline of the original component.

4.2. Extraction of semantic relationships

The morphological operators provide a means to simplify the geometric features. To properly generalize the topological relations, correct type of semantic relationships must be extracted.

The case of a mortise-and-tenon-like relationship (mortise-and-tenon for short) is illustrated in Fig. 12a). There are many variations of mortise-and-tenon. However, in general, mortises are built from concave features, such as grooves or holes, and tenons are built from convex features, such as protrusions. As a result, the extraction of a mortise-and-tenon is the extraction of the nested features of two components. In addition, the size of the mortise-and-tenon reflects the degree of connection between components in the building structure in which the smaller the size, the closer is the connection. Therefore, different levels of connection can be extracted with scale parameters in increasing order.

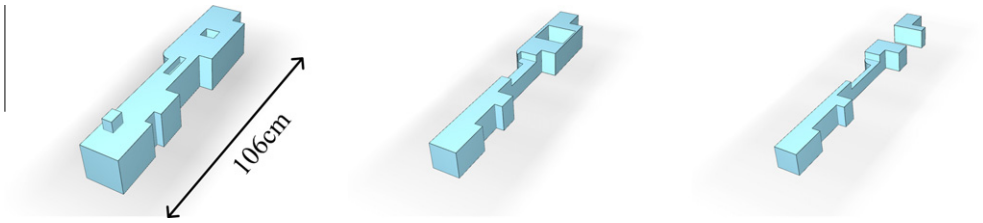

Fig. 9. Illustration of the result of the erosion (left, the original model; middle, the erosion result at scale parameter 6 cm; right, the erosion result at scale parameter 8 cm).

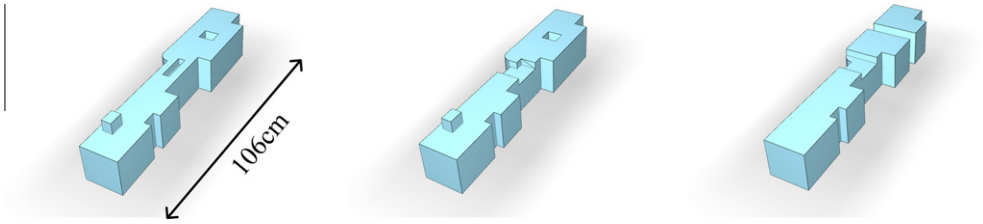

Fig. 10. Illustration of the result of opening (left, the original model; middle, the opening result at scale parameter 4 cm; right, the opening result at scale parameter 8 cm).

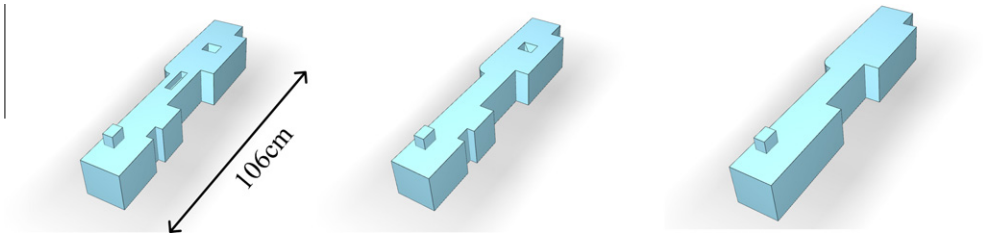

Fig. 11. Illustration of the result of closing (left, the original model; middle, the closing result at scale parameter 4 cm; right, the closing result at scale parameter 6 cm).

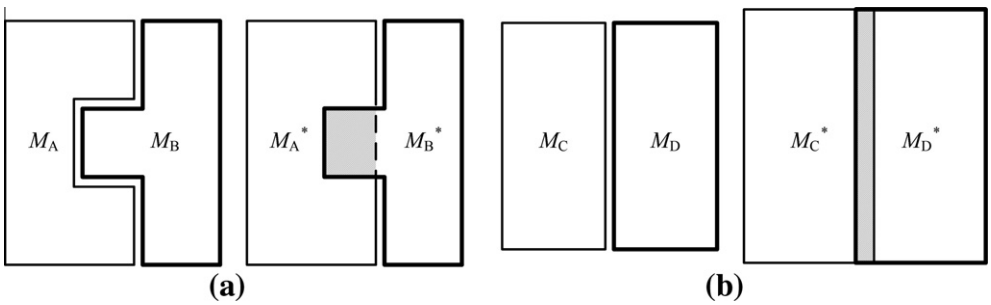

Fig. 12. Illustration of the extraction of two types of relationships: (a) mortise-and-tenon and (b) masonry.

The structure of masonry-like relationship (masonry for short) is relatively simple; contiguous components are connected, as illustrated in Fig. 12b). However, in practice, there may be gaps of small sizes between contiguous components due to the modeling error. Therefore, masonry in this paper is extended to support separated components in which the distances between the components represent the degree of connection in which the closer the distance, the closer is the connection. Additionally, the extended masonry can also be used to describe more general structures (for example, the relationships between buildings).

Based on the analysis described above, the method is proposed as follows. Given a collection of components, the morphological operators, closing and dilation, and the collision detection are combined to extract the semantic relationships. For a mortise-and-tenon, all the components are first "closed" at a given scale parameter. As a result, all the mortise features that are smaller than the structural element are filled, while the tenon features are maintained. Subsequently, connections between components are detected by searching whether any two "closed components" intersect. If intersected, the two components are treated as connected. The process is illustrated in Fig. 12a) in which M'_A and M'_B are the "closed" versions of M_A and M_B, respectively. For masonry, all the components are first "dilated" at a given scale parameter. Then, connections between the components are detected by searching whether any two "dilated components" are intersected, as illustrated in Fig. 12b), where M'_C and M'_D are the "dilated" versions of M_C and M_D, respectively. If intersected, the two components are treated as connected. In the above processes, components with different materials should not be treated as connected.

Eventually, the extracted semantic relationships of the components are recorded in the connectivity graph, as illustrated in Fig. 13, in which nodes with different colors represent components built by different materials, links represent the extracted connectivity and scale parameter $t_2 > t_1$. According to the connectivity graph, the topological relations of components can be generalized.

4.3. Component merging and feature elimination

In this step, the links of the connectivity graph are iterated. For components connected by mortise-and-tenon, the merging is realized directly by employing the 3D Boolean operator "add" with the connected components produced by the previous "closing" step. The process is illustrated in Fig. 14. For masonry, the "add" operator is used with connected components that are "dilated" by the previous step. Then, the morphological operator "erosion" (at the same scale parameter) should be used on the merged model to restore the original size of the components, as illustrated in Fig. 15.

The steps presented above are iteratively executed until all the links in the connectivity graph are visited. As a result, the topological relations are generalized by merging semantically connected components. Meanwhile, the morphological operations carried out in the extraction stage eliminate trivial features at the given scale parameter. The unified generalization of geometry and topological relations is thereby achieved.

It should be noted that new redundancy of features and facets might appear after the merging process. For example, when two components are merged, gaps between these models may produce cracks in the result, as shown in Fig. 12a). Besides, Boolean operators might also introduce redundant facets to the mesh. Therefore, post-processing of the merged components is required; this processing first deploys a closing operator at the same scale parameter to eliminate cracks in the model and then uses mesh simplification (with an appropriate threshold) to simplify coplanar facets and curved surfaces.

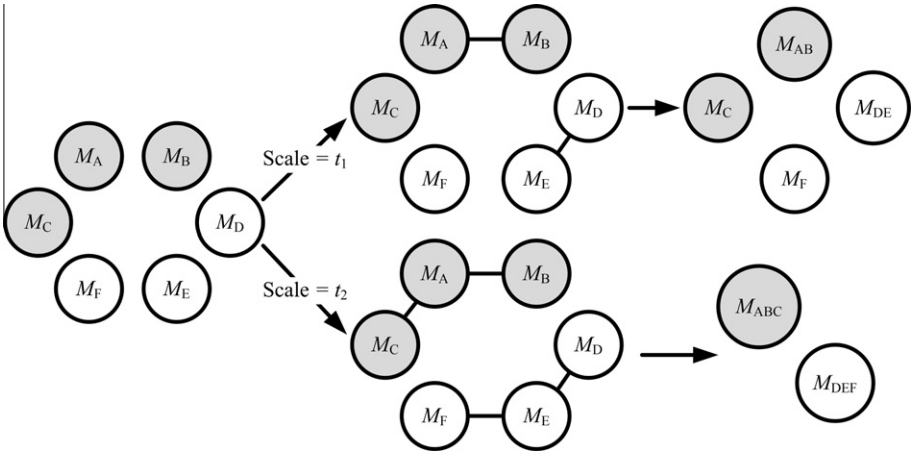

Fig. 13. Illustration of the connectivity graph and the merging of components (left, nodes represent the original components; middle, the connectivity graph extracted at two given scale parameters; right, the results of the component merging based on the connectivity graph).

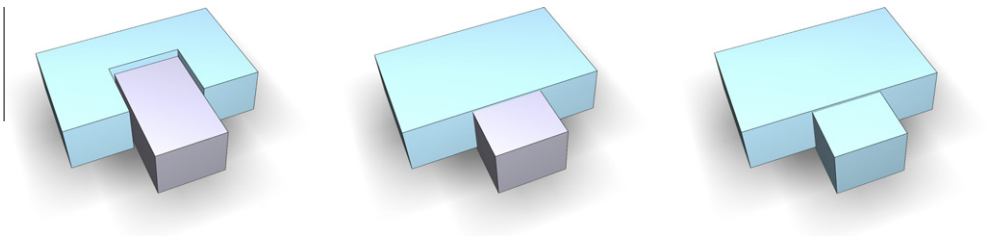

Fig. 14. Illustration of the merging process of mortise-and-tenon (left, the original model; middle, after the "closing" process, the mortise feature is "closed"; right, two intersected components are "added").

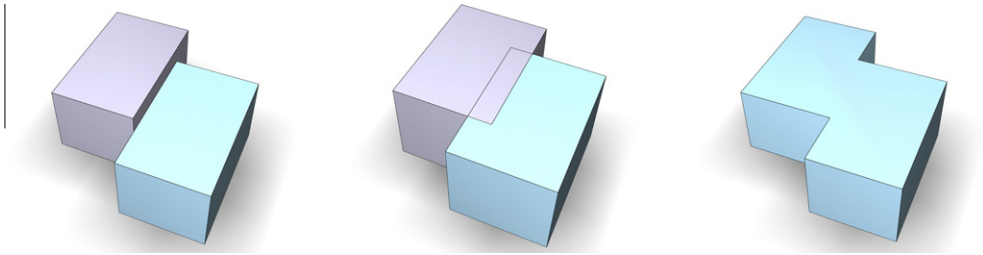

Fig. 15. Illustration of the merging process of masonry (left, the original model; middle, after the "dilation" process, both models are "expanded"; right, two intersected components are first "added" and then "eroded").

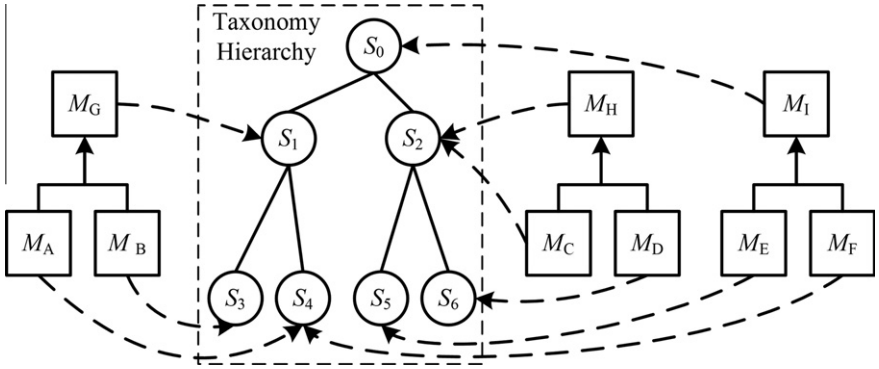

Fig. 16. Illustration of the semantic update according to the taxonomy hierarchy ($\{M_i \mid i \in A, \ldots, J\}$ represent components and $\{S_i \mid i \in \mathbb{N}\}$ represent taxonomy attributes associated with components).

4.4. Semantic update

To maintain the causal links between the LoDs produced at multiple scale parameters, the semantic information of components in LoD_{i+1} should be derived from that in LoD_i. In this paper, a typical type of semantics, namely structural taxonomy of building components, is used as an example.

As shown in Fig. 16, components M_A and M_B associate with sibling nodes S_3 and S_4 in the taxonomy hierarchy. Thus, the merged component M_G should be assigned the parent node of S_3 and S_4 (e.g., the wall should be assigned to the merging result of bricks). In another case, if two components associate with semantics at different levels of hierarchy (such as M_C and M_D in the figure), the generalized version M_H should be assigned to semantics of the higher level. This would probably occur when merging a component with a generalized component. In addition, two connected components might point to semantic nodes in different sub-trees, such as M_E and M_F in the figure. In that case, the resulting component M_I should be assigned with the lowest common ancestor, S_0 (e.g., the merging result of a wall and a roof should be a building part).

The semantic update ensures that the semantics of a component correspond to the generalization process such that the consistency of semantics in multiple LoDs can be maintained. For semantics other than structural taxonomy, corresponding method for semantic update must be devised.

5. Experiments

To validate the proposed generalization algorithm, four groups of experiments are carried out. First, building components connected by mortise-and-tenon and masonry are selected to create LoDs at different scale parameters. Then, components with both relationships are chosen to examine the constraints of semantics. Finally, the algorithm is applied to prismatic 3D city models to evaluate its applicability to the traditional dataset.

The complex 3D building model used in the experiment is a classical Chinese building, as shown in Fig. 17. This type of building is built of two parts: the timber frame and the tiled roof. Because the Dou Gong layer in the timber frame is the most intricate part of the building, parts of this layer (shown as I and II in Fig. 17) are selected for the experiment described in Section 5.1. A tiled roof in classical Chinese style is similar to other tile-based roofs around the world, and presents the structure of the masonry. In the experiment described in Section 5.2, parts of the roof's surface and ridge are selected, as shown by III and IV in Fig. 17. Because of the self-symmetry of the structure, the repeat unit of the illustrated area is used.

The application of the Minkowski sum and the Boolean operation in a 3D model is based on the Computational Geometry Algorithms Library (CGAL) package (CGAL, 2010). The mesh simplification is implemented using a half-edge collapse-based QEM. In the experiment, two control parameters, scale parameter and simplification ratio are chosen by trial and error according to the relative size of the input model. The final note is that all the LoDs are created directly from the original model, and the result is identical to those produced successively.

5.1. Generalization of the timber frame

Fig. 18 shows the selected collection of components in experimental area I. They are composed of the Ni Dao Gong (M_A and M_B), the Lu Dou (M_C and M_D), and the Gong Yan Bi (M_E), and they total five components and 3876 triangles. There are features of various sizes on each component, such as the window frame feature f_0 in M_E, the mortise features f_1, f_2, f_5, and f_7 in M_A and M_B, and the mortise features f_3, f_4, f_6 in M_C and M_D. The demonstrated features are sorted by their sizes as follows:

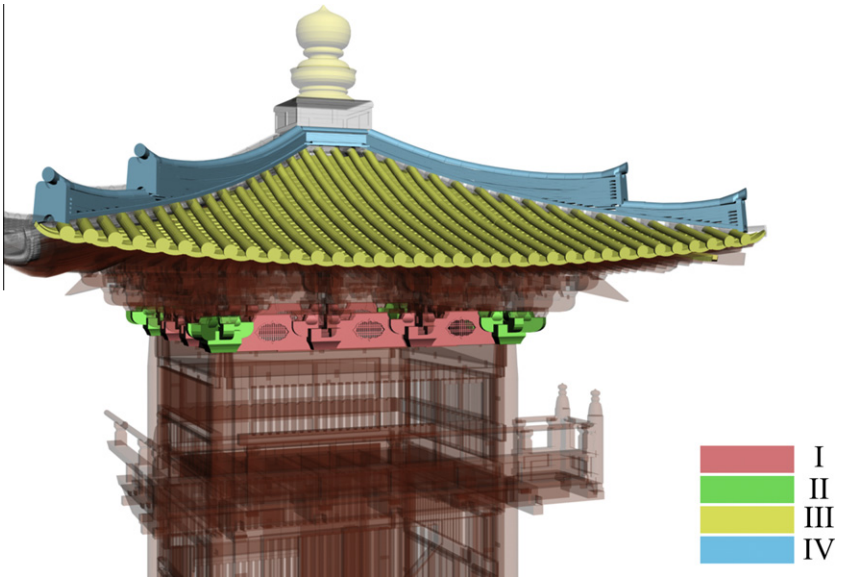

Fig. 17. Illustration of the experimental data (a Bell tower with 98,265 components and 706,978 triangles).

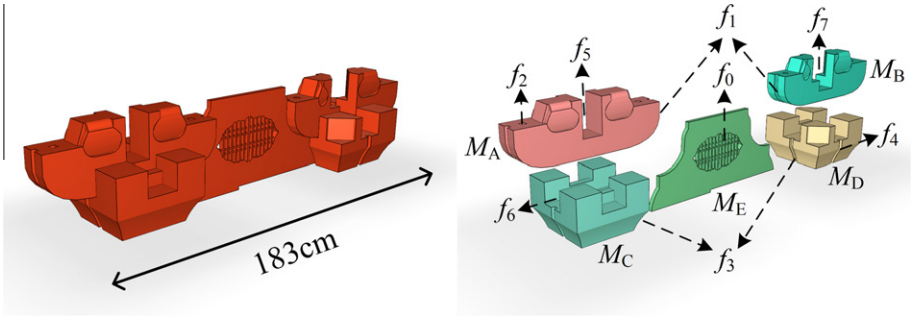

Fig. 18. Experimental data I (left, the original model; right, the exploded view illustration with pseudo material).

$$s(f_0) < s(f_1) = s(f_2) < s(f_3) < s(f_4) < s(f_5) < s(f_6) = s(f_7)$$

where $s(f_i)$ represent the smallest width of grooves in feature $\{f_i \mid i \in \mathbb{N}\}$. As discussed in Section 4.2, the degree of connection can be represented by the sizes of the joint features. Taking M_E as an example, M_E and M_A as well as M_E and M_B are connected by the mortise feature f_1 and the tenon feature in M_E. Similarly, M_E and M_C as well as M_E and M_D are connected by the mortise feature f_3 and the tenon feature in M_E. Thus the priority of connections is sorted as follows:

$$C(M_A, M_E) = C(M_B, M_E) > C(M_C, M_E) = C(M_D, M_E)$$

where $C(M_i, M_j)$ represent the priority or degree of the connection between the components M_i and M_j.

Fig. 19 shows the selected collection of components in experimental area II. They are composed of the Jiao Hua Gong (M_A), the Jiao Ni Hua Gong (M_B and M_C), and the Jiao Lu Dou (M_D), and they total four components and 2384 triangles. The demonstrated features in the figure are sorted by their sizes as follows:

$$s(f_0) = s(f_1) < s(f_2) = s(f_3) < s(f_4)$$

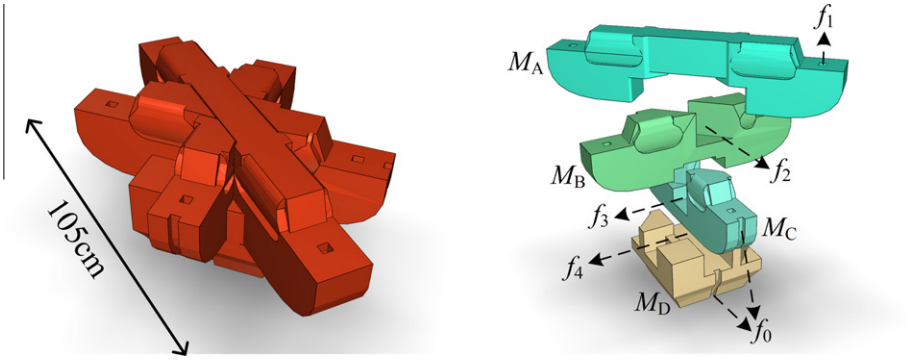

Fig. 19. Experimental data II (left, the original model; right, the exploded view illustration with pseudo material).

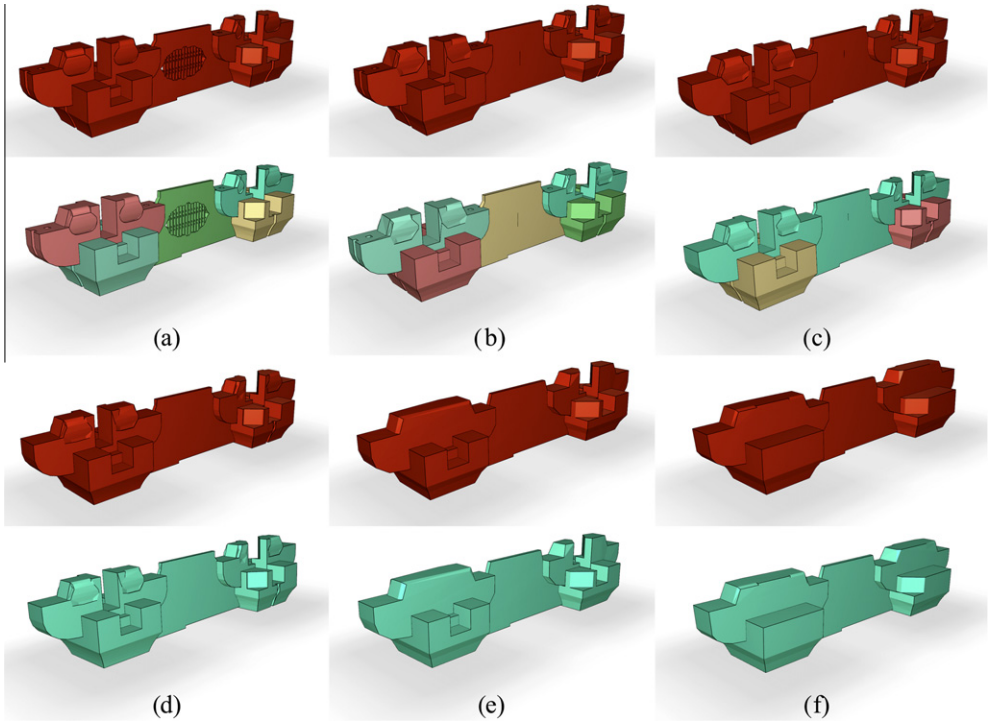

Fig. 20. The LoDs produced from experimental data I (for each LoD: above, illustration with original material; below, illustration with pseudo material).

Table 1
The statistics of the results from Fig. 20.

LoDs	*a*	*b*	*c*	*d*	*e*	*f*
Scale parameter (cm)	0	2.336	2.384	2.388	10	20
Simplification ratio	0	65%	65%	65%	70%	70%
The number of models	5	5	3	1	1	1
The number of facets	3876	1386	1330	1096	482	386

Table 2
The statistics of the results from Fig. 21.

LoDs	*a*	*b*	*c*	*d*
Scale parameter (cm)	0	4	12.1	50
Simplification ratio	0	60%	60%	65%
The number of models	4	4	2	1
The number of facets	2384	752	750	584

The priority of connections is sorted as follows:

$$C(M_A, M_B) = C(M_B, M_C) > C(M_B, M_D) = C(M_C, M_D)$$

The produced LoDs are shown in Fig. 20. Table 1 shows the statistics of the results. Fig. 20a) is the original model. When the scale parameter grows to 2.336 cm, the window frame f_0 is eliminated (Fig. 20b). At the scale parameter of 2.348 cm, the grooves f_1 and f_2 of the mortise feature are closed, which leads to the merging of M_E, M_A, and M_B (Fig. 20c). At the next scale parameter, f_3 is eliminated, which leads to the merging of the rest of the components (Fig. 20d). As the scale parameter continues to increase, larger features, such as f_4, f_5, f_6, and f_7, are gradually eliminated, as shown in Figs. 20e and 20f. As a result, the complexity of the geometry and the topological relations are progressively reduced. The results also show that because the generalization connects components and eliminates trivial details, heavier simplification (from 65% to 70%) can be adopted without affecting the appearance of the model.

The statistics of the results from experimental data II are shown in Table 2. The produced LoDs are shown in Fig. 21. Given the scale parameter of 4 cm, grooves f_0 and f_1 are closed (Fig. 21b). When the scale parameter increases to 12.1 cm, mortise features f_2 and f_3 are eliminated, which leads to the merging of M_A, M_B, and M_C (Fig. 21c). Finally, when the scale parameter increases to 50 cm, all the

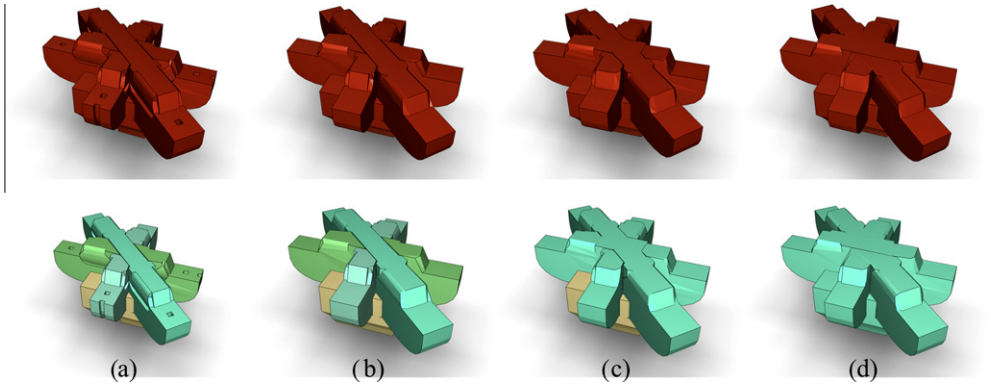

Fig. 21. The LoDs produced from experimental data II (for each LoD: above, illustration with original material; below, illustration with pseudo material).

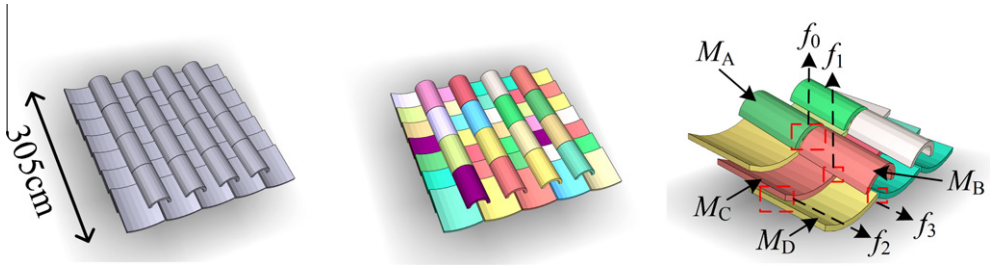

Fig. 22. Experimental data III (left, the original model; middle, the illustration with pseudo material; right, the exploded view illustration of parts of the model with pseudo material).

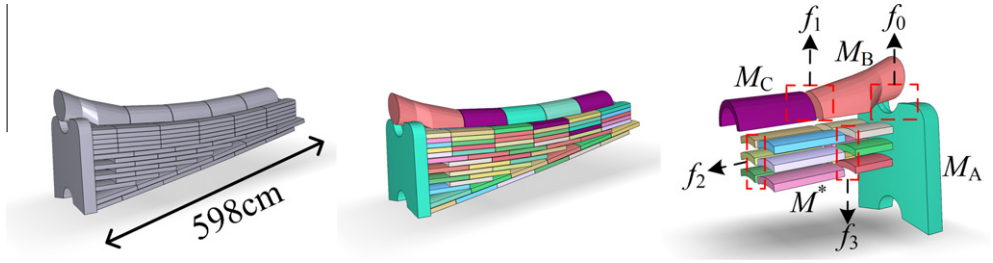

Fig. 23. Experimental data IV (left, the original model; middle, the illustration with pseudo material; right, the exploded view illustration of the parts of the model with pseudo material).

Table 3
The statistics of the results from Fig. 24.

LoDs	*a*	*b*	*c*	*d*
Scale parameter (cm)	0	0.4	8	25
Simplification ratio	0	70%	80%	80%
The number of models	51	9	1	1
The number of facets	3100	3742	2296	901

Table 4
The statistics of the results from Fig. 25.

LoDs	*a*	*b*	*c*
Scale parameter (cm)	0	3	30
Simplification ratio	0	70%	70%
The number of models	124	1	1
The number of facets	6846	2398	996

components are merged (Fig. 21d). The produced LoD model reduces 75.5% of the facets of the original model; however, the appearance is retained.

5.2. Generalization of tiled roof

Fig. 22 shows the selected collection of components in experimental area III. They consist of upper tiles (M_A and M_B) and lower tiles (M_C and M_D). The test data contain 51 components and 3100 triangles. The relationship between the tiles presents masonry features as shown by f_0, f_1, f_2, and f_3 in Fig. 22. The demonstrated features are sorted by their sizes as follows:

$$0 \approx s(f_0) = s(f_2) < s(f_1) < s(f_3)$$

where $s(f_i)$ represent the size of feature $\{f_i \mid i \in \mathbb{N}\}$, which is the smallest distance between two contagious components. Thus, $s(f_i) = 0$ indicates that two components "meet" each other. In reality, the size of the masonry should be equal to 0; however, because of the modeling error, there are always tiny gaps between tiles (intersections are also common but can be healed using an erosion operator). As a result, under some small scale parameters, two contiguous tiles may not be merged.

Fig. 23 shows the selected collection of components in the experimental area IV. They are composed of Head tiles (M_A), Ridge

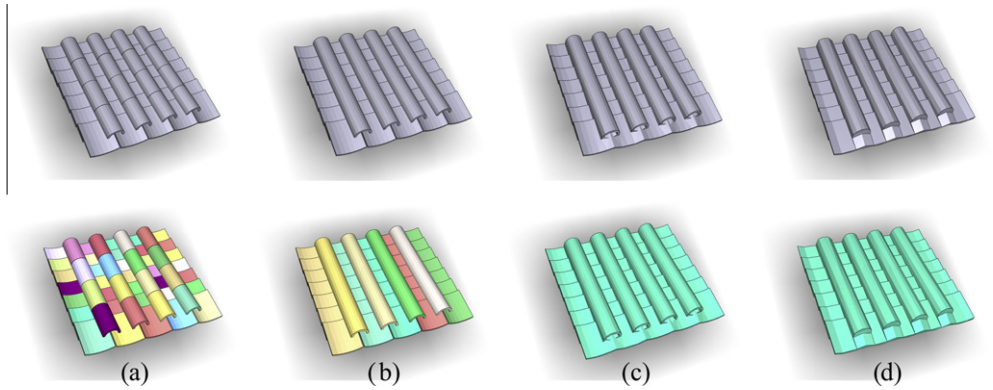

Fig. 24. The LoDs produced from experimental data III (for each LoD: above, illustration with original material; below, illustration with pseudo material).

tiles (M_B and M_C)m and Pi Shui tiles (M^*), and they total 124 components and 6846 triangles. All the components are connected by masonry features f_0, f_1, f_2, and f_3. Their sizes are all approximately 0.

The statistics of experimental data III are shown in Table 3. Fig. 24 shows the produced LoDs. When the scale parameter is 0.4 cm, which is slightly larger than 0, the features f_0 and f_2 are eliminated. The results show that each column of tiles is merged

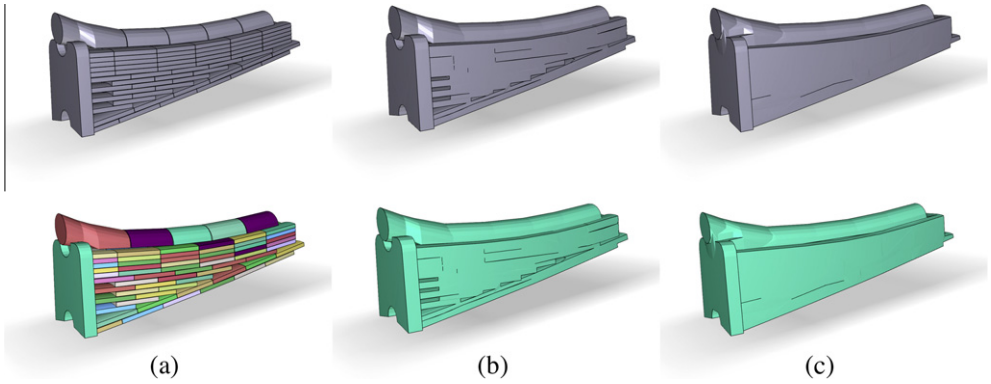

Fig. 25. The LoDs produced from experimental data IV (for each LoD: above, illustration with original material; below, illustration with pseudo material).

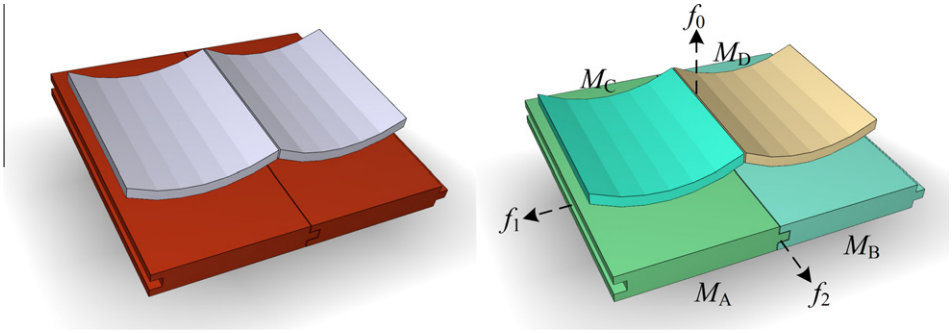

Fig. 26. Tiles and the cornice board (left, the original model; right, the illustration with pseudo material).

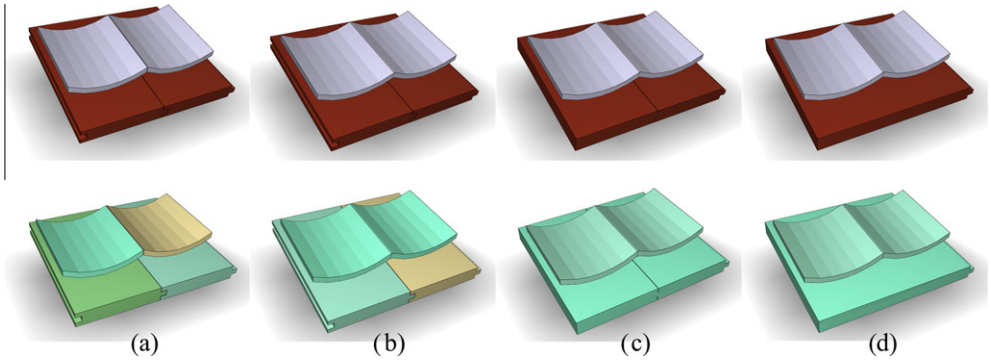

Fig. 27. The produced LoDs for the tiles and the cornice board: (a) the original model; (b) the two tiles are merged; (c) the two cornice boards are merged; and (d) the elimination of redundant features (for each LoD: above, illustration with original material; below, illustration with pseudo material).

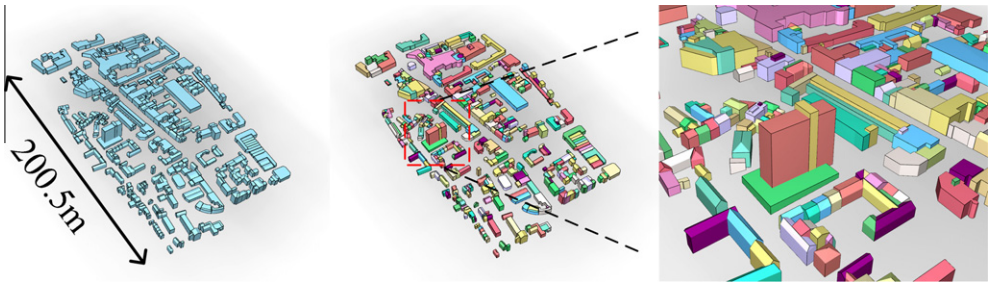

Fig. 28. Experimental data V (left, the original model; middle, the illustration with pseudo material; right, the zoom-in of a local area).

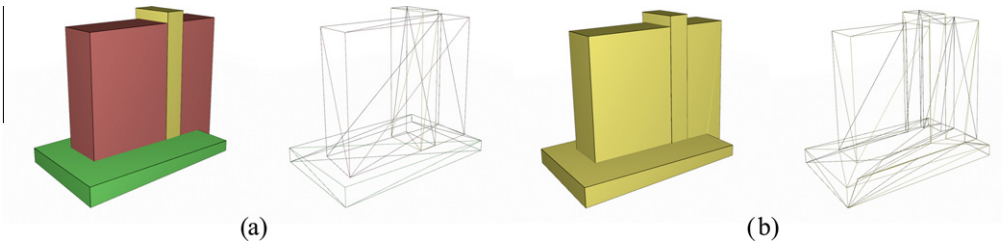

Fig. 29. The results of the topology correction: (a) the original building model (three models and 36 facets); (b) the building model with the corrected topology (one model and 78 facets).

Table 5
The statistics of the results from Fig. 30.

LoDs	*a*	*b*	*c*	*d*	*e*	*f*
Scale parameter (m)	0	0.01	0.5	3	4	6
Simplification ratio	0	60%	60%	64%	70%	70%
The number of models	418	186	81	30	16	3
The number of facets	7754	9616	8935	7858	6231	5949

into one component (Fig. 24b). At a scale parameter of 8 cm, features f_1 and f_3 are eliminated. Then, all the contiguous components are merged (Fig. 24c). When the scale parameter increases, the tube-like hollow space formed by the merging of upper and lower tiles is filled (Fig. 24d). The data volume decreases to 29% of the original model.

The statistics of experiment IV are shown in Table 4. The produced LoDs are illustrated in Fig. 25. To omit the influence of small gaps between tiles, a relatively larger initial scale parameter of 3 cm is chosen. This scale parameter directly merges all the components into one, as shown in Fig. 25b, but the holes formed by the tiles are maintained. At this stage of generalization, the roof ridge is modeled at 35% of the original data amount. When the scale parameter increases to 30 cm, all the holes in the model are filled. At this point, a similar-looking roof ridge with 14.5% of the original facets is obtained (Fig. 25c).

5.3. Generalization with the semantics constraint

In this experiment, a collection of components with different materials is selected to validate the effectiveness of the semantics constraint. Fig. 26 shows part of the tiled roof (M_C and M_D) and the timber cornice boards (M_A and M_B) that support the tile. Because of the different materials, these models present different semantic relationships; that is, M_A and M_B are connected by mortise-and-tenon features, f_1 and f_2, and M_C and M_D are connected by the masonry feature, f_0. Features are sorted by their sizes as follows:

$$0 \approx s(f_0) < s(f_1) = s(f_2)$$

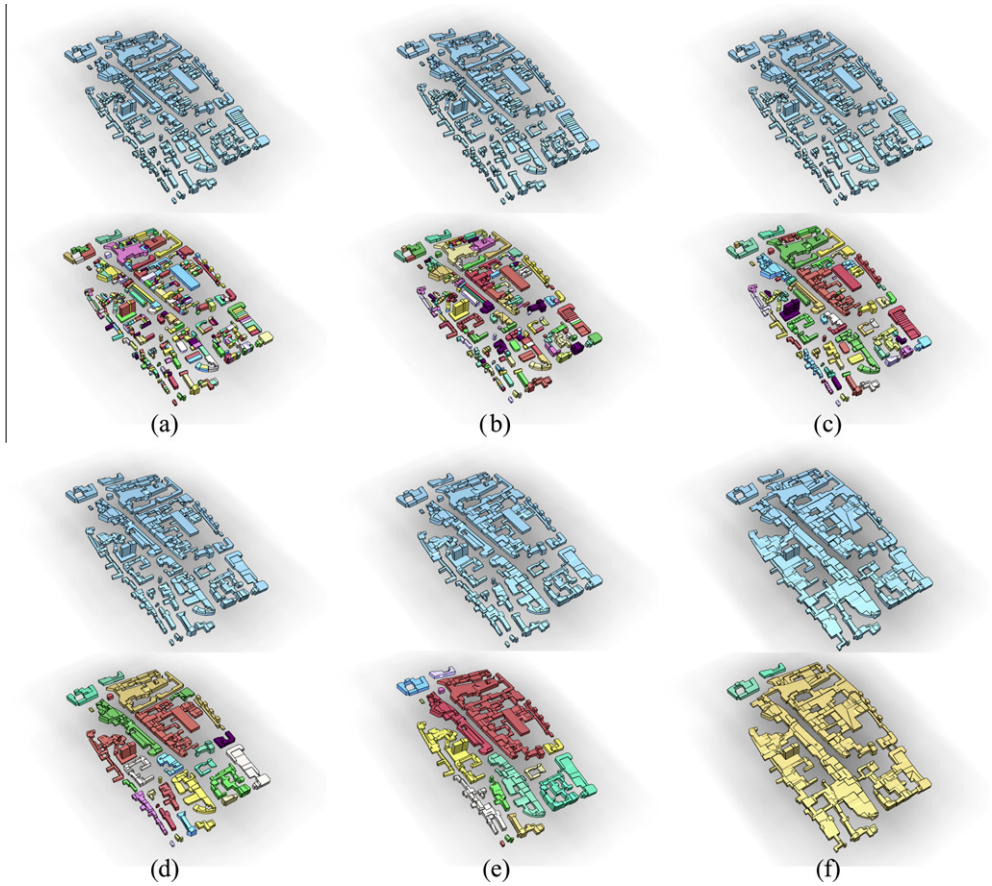

Fig. 30. The LoDs produced from experimental data V (for each LoD: above, illustration with original material; below, illustration with pseudo material).

In the extraction of semantic relationships, the algorithm automatically switches between different routines for mortise-and-tenon and masonry according to the material of the component. The assumption made here is that all timber frame components are connected by mortise-and-tenon and all tiles are connected by masonry.

Fig. 27 shows the generalization results of the test data. In the first LoD, the smallest masonry feature f_0 is eliminated, and the tiles M_C and M_D are merged (Fig. 27b). At the next scale parameter, the mortise features f_1 and f_2 are eliminated so that the components M_A and M_B are merged (Fig. 27c). In the last LoD, the gaps produced in the previous step are closed by employing a closing operator, and the tile and the board remain isolated (Fig. 27d).

5.4. Generalization of 3D city models

Finally, to verify the applicability of the proposed algorithm in more general cases, a sample dataset, as shown in Fig. 28, is selected as experimental data V. These data are from part of the 3D city models of the Ordnance Survey Great Britain (CityGML, 2011). The dataset contains 418 models and 7754 triangles.

As discussed in Section 4.2, the semantic relationships between buildings can be treated as the "extended masonry". However, due to the method of 2.5D modeling, one building may be presented as three intersected blocks, as shown in Fig. 29a). Thus, it would be good if the proposed algorithm could correct this topological error.

Table 5 shows the statistics of the generalized LoDs illustrated in Fig. 30. At a very small scale parameter of 0.01 m, all the intersected models are merged, while different buildings remain separated. A sample is shown in Fig. 29b). After topology correction, the number of 3D city models decreases to 186 which is the actual building number. However, it should be noted that the topology-corrected model may introduce more details, and this will lead to the growth of facet numbers.

As the scale parameter increases, the number of building models declines, as shown in Fig. 30. Finally, buildings are merged into three building groups at the scale parameter of 6 m. The number of facets decreases moderately to 60% of the topology-corrected model.

6. Discussion

6.1. Analysis of the experimental results

The experimental results show the effectiveness of the proposed algorithm for the generalization of complex 3D building models. At a given scale parameter, the algorithm eliminates the

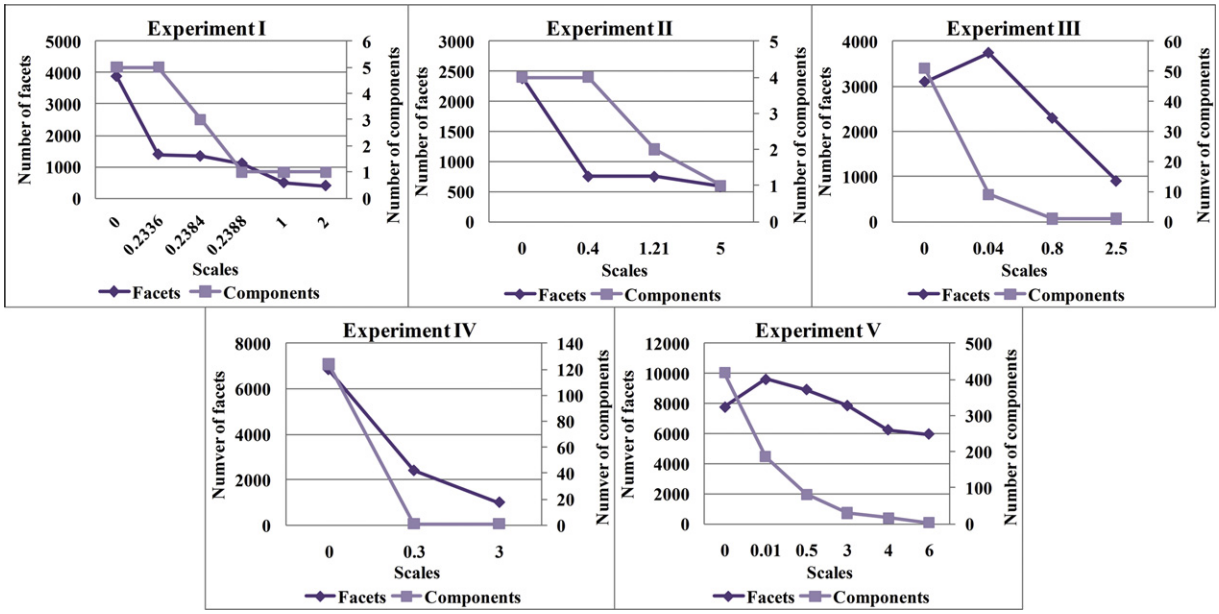

Fig. 31. The statistics of the results of five experiments.

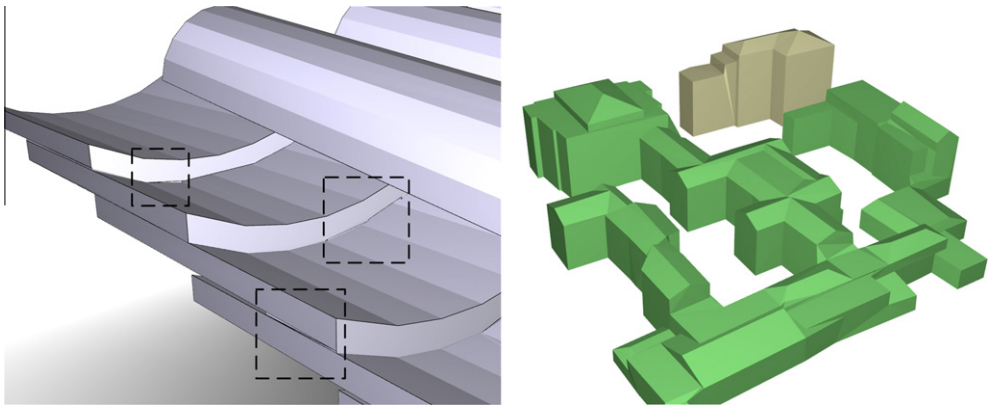

Fig. 32. Illustration of the generalization results of masonry (left, partial connections between tiles; right, irregular roof structure).

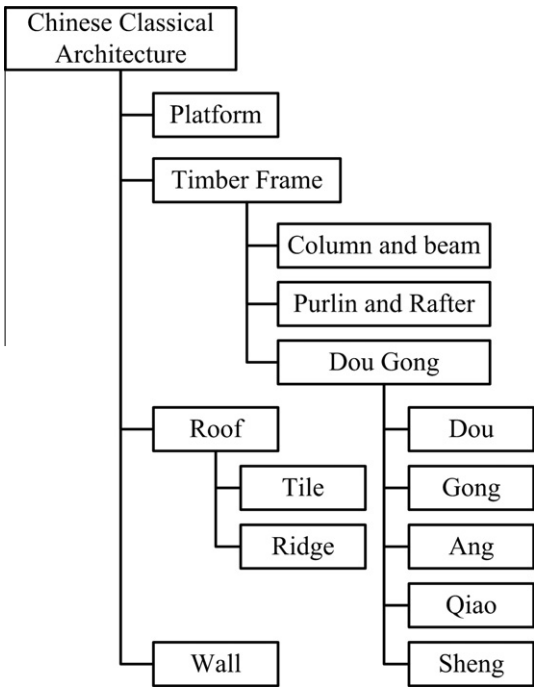

Fig. 33. A brief taxonomy hierarchy of classical Chinese architecture.

insignificant features and generalizes the topological relations and the semantics properly by incorporating the semantic relationships.

As shown in Fig. 31, the greatest decrease of facets in experiments I and II in Section 5.1 is found at the first LoD. The reason is that the elimination of small features in the timber frame component enables heavier simplification without introducing significant artifacts. In successive LoDs, the merging of components further reduces facets, which also helps to maintain the general shape of the model during mesh simplification.

In the third experiment (tiled roof) in Section 5.2, generalization at a small scale parameter might partly connect components, as shown in Fig. 32(left). This is due to the unparalleled distribution of components derived from the modeling phase. As a result, the number of facets is increased by 20% when the scale parameter is 0.4 cm, as shown in Fig. 31. However, when the scale parameter further increases, the components are fully connected, and the number of facets then decreases. The result of experiment IV avoids showing similar results by adopting a larger initial scale parameter.

In experiment V, the exponential decrease in components and the well kept building structure shows that the topological relations of buildings are successfully generalized. However, the reduction in facet numbers is less apparent. The reason is that the irregular roof structures of the building produce rugged surfaces in the results, as shown in Fig. 32(right). Therefore, for practical use, these features should be eliminated with morphological operators such as opening or by inverting the normal of each facet first and conducting closing operation sequentially (El-Sana and Varshney, 1998).

Because the building components used in the experiment do not contain taxonomy attributes, the semantic update is not evaluated in the experiment. However, the feasibility of such a process can be understood intuitively. According to the brief taxonomy hierarchy of the classical Chinese architecture shown in Fig. 33, the semantics of the merged components can be easily assigned based on the approach described in Section 4.4.

6.2. Comparison study

Because of its generality and wide acceptance in the application of model simplification, the classic QEM method is chosen for comparison (Garland, 1999).

The comparison of the results of the timber frame component is shown in Fig. 34, and the comparison of the results of tiled component is shown in Fig. 35. It is obvious that the proposed generalization method produces better results even if the results of QEM contain more facets. The main reason is that our approach properly

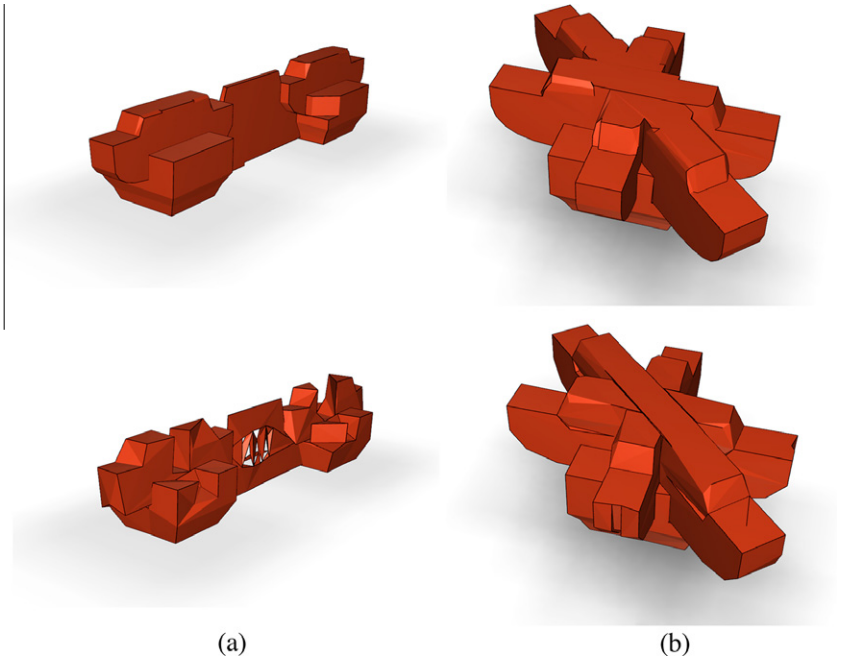

Fig. 34. Comparison with QEM simplification. (a) Results of experimental data I: above, by the proposed method (386 facets); below, by QEM simplification (386 facets). (b) Results of experimental data II: above, by the proposed method (584 facets); below, by QEM simplification (584 facets).

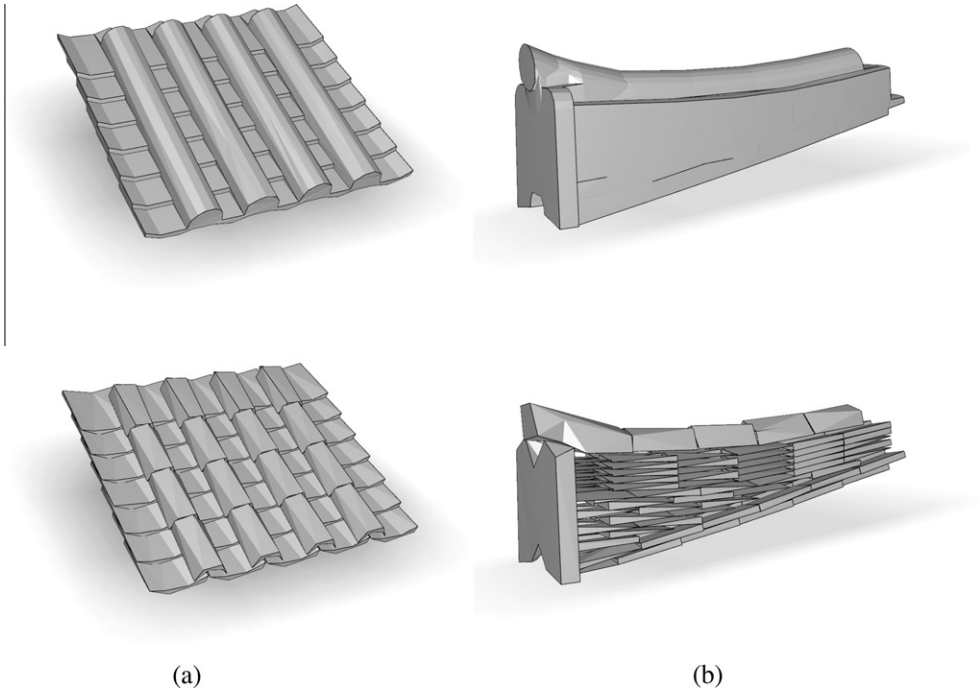

Fig. 35. Comparison with QEM simplification. (a) Results of experimental data III: above, by the proposed method (901 facets); below, by QEM simplification (901 facets). (b) Results of experimental data IV: above, by the proposed method (996 facets); below, by QEM simplification (996 facets).

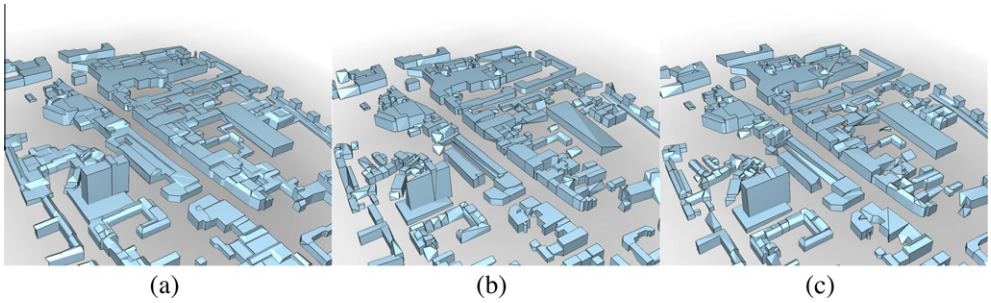

Fig. 36. Comparison of the results of experimental data V with QEM simplification: (a) by the proposed method (6231 facets); (b) by QEM simplification of original models (6231 facets); (c) by QEM simplification of topology-corrected models (6231 facets).

generalized the topological relations together with the geometric features. The results of 3D city models are compared with two cases of simplification. The first is the simplification of the original models (Fig. 36b), and the second is the simplification of topology-repaired models (Fig. 36c). Although the topology-repaired models produce better results than the original ones, neither of these results could preserve the shapes of the buildings. In contrast, the proposed generalization algorithm can maintain most of the man-made features (such as perpendicular and parallel facets), and the general shape of building group is also retained.

6.3. Computational efficiency

The proposed method aims at the offline generalization of complex 3D building models; the computational efficiency is therefore roughly evaluated. All the experiments are conducted on a workstation with Intel Xeon w5580 CPU at 3.2 GHz. The least time cost is the experiment II in Section 5.1, which requires approximately 10 min producing an LoD model. The slowest is experiment V in Section 5.4, which requires approximately about 40 min producing a result. The maximum memory usage is around 0.8–1.4 GB. Dividing the algorithm into four parts, namely the morphological operation, the collision detection, the Boolean operation and the mesh simplification, the Minkowski sum used in morphological operation requires nearly 80% of the total computing time. However, because the Minkowski sum in CGAL is implemented based on the convex segmentation of the polyhedron, a parallel paradigm can be employed to alleviate the bottleneck. Alternately, a more efficient method (mentioned in Section 4.1) can be used.

7. Conclusions and outlook

A method based on mathematical morphology is proposed in this paper with the aim of automatic generalization of complex 3D building models. This method can process any closed two-manifold mesh by exploring the generality provided by the 3D Minkowski sum and the 3D Boolean operation. The most important characteristic of this method is its capacity to maintain the consistency of geometry, topological relations, and semantics in multiple LoDs by accounting for the semantic relationships of building components. Experiments on both complex 3D building models and 3D city models prove the effectiveness of the proposed method.

Future research should include the implementation of the proposed method to other kind of building models such as BIM and CityGML and the automatic extraction of semantic information from complex 3D building models to provide better generalization constraints. More guidelines, such as the city infrastructures as mentioned in Chang et al. (2008), can be further included to produce optimal results for city models. Another possible research topic would be the automatic selection of the scale parameters in an adaptive manner (Erikson and Manocha, 1999).

Acknowledgements

The authors thank anonymous reviewers and Professor Sisi Zlatanova and Professor Thomas H. Kolbe for their helpful suggestions. Thanks to Sébastien Loriot for the kind help on the implementation of CGAL. This study is supported by the National Basic Research Program of China (973 Program, Nos. 2010CB731801 and 2011CB302306) and the National Natural Science Foundation of China (41171311 and 41021061).

References

Anders, K.H., 2005. Level of detail generation of 3D building groups by aggregation and typification. In: Proceedings of the 22nd International Cartographic Conference. Mapping Approaches into a Changing World, A Coruña, Spain, 9–16 July, 8 p (on CD-ROM).

Babic, B., Nesic, N., Miljkovic, Z., 2008. A review of automated feature recognition with rule-based pattern recognition. Computers in Industry 59 (4), 321–337.

CGAL, 2010. Computational geometry algorithms library. <http://www.cgal.org/> (accessed 18.07.11).

Chang, R., Butkiewicz, T., Ziemkiewicz, C., Wartell, Z., Ribarsky, W., Pollard, N., 2008. Legible simplification of textured urban models. IEEE Computer Graphics and Applications 28 (3), 27–36.

CityGML, 2011. Official Website of CityGML. <http://www.citygml.org/> (accessed 18.07.11).

Cook, R.L., Halstead, J., Planck, M., Ryu, D., 2007. Stochastic simplification of aggregate detail. ACM Transactions on Graphics 26 (3) (Article No. 79).

Damen, J., Van Kreveld, M., Spaan, B., 2008. High quality building generalization by extending morphological operators. In: Proceedings of the 11th ICA Workshop on Generalisation and Multiple Representation, Montpellier, France, 20–21 June, 12 p (on CD-ROM).

Du, Z., Zhu, Q., Zhao, J., 2008. Perception-driven simplification methodology of 3D complex building models. In: International Archives of Photogrammetry, Remote Sensing and Spatial Information Sciences, vol. 37 (Part B5), 8 p (on CD-ROM).

Egenhofer, M.J., Robert, D.F., 1991. Point-set topological spatial relations. International Journal of Geographical Information System 5 (2), 161–174.

El-Sana, J., Varshney, A., 1998. Topology simplification for polygonal virtual environments. IEEE Transactions on Visualization and Computer Graphics 4 (2), 133–144.

Erikson, C., Manocha, D., 1999. GAPS: general and automatic polygonal simplification. In: Proceedings of the 1999 Symposium on Interactive 3D Graphics, Atlanta, Georgia, United States, 26–29 April, pp. 79–88.

Fan, H., Meng, L., Jahnke, M., 2009. Generalization of 3D buildings modelled by CityGML. In: Sester, M., Paelke, V., Bernard, L. (Eds.), Advances in GIScience: Lecture Notes in Geoinformation and Cartography. Springer-Verlag, Berlin/Heidelberg, pp. 387–405.

Fogel, E., Halperin, D., 2007. Exact and efficient construction of Minkowski sums of convex polyhedra with applications. Computer-Aided Design 39 (11), 929–940.

Forberg, A., 2007. Generalization of 3D building data based on a scale-space approach. ISPRS Journal of Photogrammetry and Remote Sensing 62 (2), 104–111.

Garland, M., Heckbert, P.S., 1997. Surface simplification using quadric error metrics. In: Proceedings of the 1997 ACM SIGGRAPH, Los Angeles, California, United States, 3–8 August, pp. 209–216.

Garland, M., 1999. QSlim. <http://www.cs.cmu.edu/~garland/quadrics/qslim.html/> (accessed 23.12.11).

Glander, T., Döllner, J., 2007. Techniques for generalizing building geometry of complex virtual 3D city models. In: Oosterom, P., Zlatanova, S., Penninga, F., Fendel, E.M. (Eds.), Advances in 3D Geoinformation Systems: Lecture Notes in Geoinformation and Cartography. Springer-Verlag, Berlin/Heidelberg, pp. 381–400.

Gobbetti, E., Kasik, D., Yoon, S., 2008. Technical strategies for massive model visualization. In: Proceedings of the 2008 ACM Symposium on Solid and Physical Modeling. Stony Brook, New York, 2–4 June, pp. 405–415.

Gröger, G., Kolbe, T.H., Czerwinski, A., Nagel, C., 2008. Opengis city geography markup language (citygml) encoding standard. Version 1.0.0., Open Geospatial Consortium, OGC Doc. No. 08-007r1.

Guercke, R., Zhao, J., Brenner, C., Zhu, Q., 2010. Generalization of tiled models with curved surfaces using typification. In: Proceedings of the Joint International Conference on Theory, Data Handling and Modelling in GeoSpatial Information Science, Hong Kong, China, 26–28 May, 9 p (on CD-ROM).

Jang, J., Wonka, P., Ribarsky, W., Shaw, C.D., 2006. Punctuated simplification of man-made objects. The Visual Computer 22 (2), 136–145.

Kada, M., 2002. Automatic generalisation of 3D building models. International Archives of Photogrammetry, Remote Sensing and Spatial Information Sciences 34 (Part 4), 243–248.

Kada, M., 2007. Scale-dependent simplification of 3D building models based on cell decomposition and primitive instancing. In: Winter, S., Duckham, M., Kulik, L., Kuipers, B. (Eds.), Spatial Information Theory: Lecture Notes In Computer Science. Springer, Berlin/Heidelberg, pp. 222–237.

Lindeberg, T., 1994. Scale-space Theory in Computer Vision. Kluwer Academic Publishers/Springer, Dordrecht, The Netherlands.

Luebke, D., Erikson, C., 1997. View-dependent simplification of arbitrary polygonal environments. In: Proceedings of the 1997 ACM SIGGRAPH, Los Angeles, California, United States, 3–8 August, pp. 199–208.

Luebke, D., Reddy, M., Cohen, J.D., Varshney, A., Watson, B., Huebner, R., 2003. Level of Detail for 3D Graphics. Morgan Kaufmann, San Francisco.

Mayer, H., 2005. Scale-spaces for generalization of 3D buildings. International Journal of Geographical Information Science 19 (8), 975–997.

Mehra, R., Zhou, Q., Long, J., Sheffer, A., Mitra, N.J., 2009. Abstraction of man-made shapes. ACM Transactions on Graphics 28 (5), 1–10.

Meng, L., Forberg, A., 2006. 3D building generalisation. In: Mackaness, W., Ruas, A., Sarjakoski, T. (Eds.), Challenges in the Portrayal of Geographic Information: Issues of Generalisation and Multi Scale Representation. Elsevier Science Ltd., pp. 211–232.

Nooruddin, F.S., Turk, G., 2003. Simplification and repair of polygonal models using volumetric techniques. IEEE Transactions on Visualization and Computer Graphics 9 (2), 191–205.

Peternell, M., Steiner, T., 2007. Minkowski sum boundary surfaces of 3D-objects. Graphical Models 69 (3–4), 180–190.

Rau, J., Chen, L., Tsai, F., Hsiao, K., Hsu, W., 2006. LOD generation for 3D polyhedral building model. In: Rau, J., Chen, L., Tsai, F., Hsiao, K., Hsu, W. (Eds.), Advances in Image and Video Technology: Lecture Notes in Computer Science. Springer, Berlin/Heidelberg, pp. 44–53.

Ribelles, J., Heckbert, P.S., Garland, M., Stahovich, T., Srivastava, V., 2001. Finding and removing features from polyhedra. In: Proceedings of the 2001 ASME Design Engineering Technical Conferences, Pittsburgh, PA, USA, 9–12 September, 10 p.

Sester, M., 2007. 3D Visualization and Generalization. In: Proceedings of the 51st Photogrammetric Week, Stuttgart, Germany, 3–7 September, pp. 285–295.

Thakura, A., Banerjeea, A.G., Gupta, S.K., 2009. A survey of CAD model simplification techniques for physics-based simulation applications. Computer-Aided Design 41 (2), 65–80.

Thiemann, F., Sester, M., 2004. Segmentation of buildings for 3D-generalisation. In: Proceedings of the 7th ICA Workshop on Generalisation and Multiple Representation, Leicester, UK, 20–21 August, 7 p (on CD-ROM).

Zhu, Q., Zhao, J., Du, Z., Liu, X., Zhang, Y., 2009. Perceptually guided geometrical primitive location method for 3D complex building simplification. International Archives of Photogrammetry, Remote Sensing and Spatial Information Sciences 38 (Part C3), 3–4 (on CD-ROM).